Theoretical Study of the Reaction of CH_3 with HOCO Radicals†

Hua-Gen Yu

Department of Chemistry, Brookhaven National Laboratory, Upton, New York 11973-5000

Joseph S. Francisco*

Department of Chemistry, Purdue University, West Lafayette, Indiana 47907-2084

Received: November 4, 2008; Revised Manuscript Received: January 5, 2009

The reaction of HOCO radicals with CH_3 radicals is examined using the coupled cluster method to locate and optimize the critical points on the ground-state potential energy surface. The results show that the CH_3 + HOCO reaction can produce both the H_2O + CH_2CO and the CH_4 + CO_2 products through acetic acid and enediol intermediates. Direct ab initio dynamics calculations determine the thermal rate coefficients to be $k(T/\mathrm{K}) = 3.24 \times 10^{-11} T^{0.1024}$ in $\mathrm{cm^3 \cdot molec^{-1} \cdot s^{-1}}$ at $T \leq 1000$ K for the overall reaction. In addition, the product branching ratio of (H_2O + CH_2CO) to (CH_4 + CO_2) is predicted to be $R_{H_2O/CH_4}(T/\mathrm{K}) = 1.52 + (1.95 \times 10^{-4})T$ using RRKM theory. Both the thermal rate coefficients and the product branching ratios are weakly temperature dependent.

Introduction

The reactions of methyl radicals are important in the combustion of hydrocarbons and have been the subject of numerous experimental and theoretical studies.[1−20] Given the importance of the role of HOCO radicals[21−40] in combustion processes for converting CO to CO_2, little is known about how HOCO radicals react with one of the essential intermediates in hydrocarbon combustion reactions, that is, methyl radicals. The products resulting from the reaction of HOCO radical with methyl radicals is not known. Several reaction channels are thermodynamically accessible in combustion environments[41−43]

$$CH_3 + HOCO \rightarrow CH_4 + CO_2 \quad \text{(R1)}$$

$$\rightarrow H_2O + CH_2CO \quad \text{(R2)}$$

$$\rightarrow CO + CH_3OH \quad \text{(R3)}$$

$$\rightarrow {}^{1/3}CH_2 + HCOOH \quad \text{(R4)}$$

$$\rightarrow OH + CH_3CO \quad \text{(R5)}$$

A general trend of reactions involving HOCO radical with atoms[44−47] such as H, O, and Cl is that HOCO is very reactive with these species and these reactions involve a transfer of a hydrogen atom from the HOCO radical. Thermodynamically, hydrogen atom transfer from HOCO, reaction R1, is favored over hydrogen atoms transfer from the methyl group, reaction R4. Which of these reactions is kinetically favored is not known.

Because the methyl radical is another important species in combustion experiments, the present work examines the essential stationary points on the CH_3 + HOCO potential energy surface using ab initio methods, and molecular dynamics simulations are used to study the reaction mechanism, the lifetime of intermediates involved in the mechanism, and the thermal rate coefficient for the reaction in the temperature range of 200 to 1000 K.

Computational Method

The stationary points for the CH_3 + HOCO reaction on the singlet ground potential energy surface were computed using two levels of theory. The first one was Møller−Plesset second-order perturbation theory (MP2)[48,49] method with the augmented Dunning correlation-consistent,[50−52] aug-cc-pVDZ, basis set. This method was used in preliminary searches for minima and transition states. Full geometry optimizations were performed using Schlegel's method[53] with tolerances of better than 0.001 Å for bond lengths and 0.01° for angles and with a self-consistent field convergence of at least 10^{-9} of the density matrix. The residual root-mean-square (rms) forces were $< 10^{-4}$ au. Vibrational frequency calculations were performed to determine whether a critical point was a minimum or a transition state: all positive frequencies for a minimum or one imaginary frequency (a first-order saddle point) for a transition state. The Hessian matrices from the optimizations were then employed in refining the minima and transition states using the coupled-cluster method including single and double excitations along with a perturbative correction for triple excitations[54,55] and the aug-cc-pVDZ basis set, that is, CCSD(T)/aug-cc-pVDZ. The eigenvalue following method was used in the CCSD(T) calculations. Vibrational frequency calculations were repeated to confirm whether the critical point was a minimum or a transition state. The energies and structures of these stationary points were further optimized using the CCSD(T)/aug-cc-pVTZ method. The final energies were improved using the CCSD(T)/aug-cc-pVQZ method using the aug-cc-pVTZ optimized geometries.

Dynamics calculations were carried out using the DualOrthGT program,[56−58] where the energies and forces used in trajectory propagations were evaluated using the CAS(4,6)/6-31G(d) method[59] on the fly. As usual, trajectories were propagated with a time step of 0.34 fs for a set of randomly sampled initial conditions, where only the collision energy was held at a fixed value. The CAS(4,6) method contains four active electrons and six valence orbitals. Two active electrons are the unpaired electrons in CH_3 and HOCO and will form a σ C−C bond in CH_3COOH. The other two electrons are those in the π orbital

† Part of the special issue "George C. Schatz Festschrift".

* To whom correspondence should be addressed. E-mail: francisc@purdue.edu. Fax: 765-494-0239.

10.1021/jp809730j CCC: $40.75
Published on Web 02/09/2009

TABLE 1: Electronic Energies (au) of Stationary Points for the CH_3 + HOCO Reaction

	MP2	CCSD(T)		
species	aug-cc-pVDZ	aug-cc-pVDZ	aug-cc-pVTZ	aug-cc-pVQZ
Reactant				
CH_3	−39.70095	−39.72471	−39.76366	−39.77334
HOCO	−188.67538	−188.69550	−188.85189	−188.90071
Product				
H	−0.4993343	−0.4993343	−0.4998212	−0.4999483
$^1CH_2$	−39.00216	−39.03157	−39.06459	−39.07300
CH_4	−40.37082	−40.39582	−40.44093	−40.45172
OH	−75.56772	−75.58408	−75.64559	−75.66449
H_2O	−76.26339	−76.26706	−76.34233	−76.36357
CO_2	−188.17746	−188.18606	−188.34059	−188.38954
CH_2CO	−152.21290	−152.23869	−152.36910	−152.40759
CH_3CO	−152.78315	−152.81732	−152.94782	−152.98618
CH_2COOH	−227.86076	−227.91055	−228.103407	−228.16119
HC(O)OH	−189.33465	−189.35619	−189.51777	−189.56765
Intermediate				
$CH_3C(O)OH$ (**M₁**)	−228.53557	−228.57253	−228.77160	−228.83126
$CH_2C(OH)_2$ (**M₂**)	−228.48948	−228.52767	−228.72807	−228.78830
Transition State				
$\mathbf{TS_{H_2O}}$	−228.41731	−228.44679	−228.64416	−228.70317
$\mathbf{TS_{CH_4}}$	−228.41845	−228.45029	−228.65054	−228.70981
$\mathbf{TS_{iso}}$	−228.41704	−228.45194	−228.65221	−228.71181
$\mathbf{TS_{isw}}$	−228.41763	−228.45271	−228.65323	−228.71251

of HOC═O. Except for the corresponding occupied orbitals, the LUMO (lowest unoccupied molecular orbital) of CH_3 and the LUMO and SUMO (second-lowest unoccupied molecular orbital) of HOCO are included in the set of six active orbitals. The orientation, rotational energy, and vibrational phases of reactants were selected according to the canonical ensemble at $T = 298$ K. The initial center-of-mass distance between the CH_3 and HOCO reactants was set to be $\rho_0 = \sqrt{R_0^2+b^2}$ with $R_0 = 14.5a_0$, where $b = \xi^{1/2}b_{max}$ is the impact parameter, ξ is a uniformly distributed random number in (0,1), and b_{max} is the maximum impact parameter. In this work, to save CPU time, all trajectories were terminated before or at a simulation time of 1.0 ps. This time is sufficiently long to separate reactive trajectories from nonreactive ones. At a time of 1.0 ps, those reactive trajectories are always trapped in a deep potential well as intermediate complexes CH_3COOH, which will eventually dissociate into products at some later time owing to the fact that the exit barriers, on the basis of our ab initio calculations, apparently locate below the reactant asymptote.

Reaction cross sections at a given collision energy of E_T are calculated to be[60]

$$\sigma_r(E_T) = \pi b_{max}^2 P_r \tag{1}$$

with the reaction probability

$$P_r = N_r/N \tag{2}$$

where N_r is the number of reactive trajectories from a total of N trajectories. The errors of calculated cross sections can be written as

$$\Delta\sigma_r(E_T) = \pi b_{max}^2 \left(\frac{N_r(N-N_r)}{N^3}\right)^{1/2} \tag{3}$$

The thermal rate constants are given by

$$k(T) = g_e\left(\frac{8}{\pi\mu(k_BT)^3}\right)^{1/2}\int_0^\infty E_T\sigma_r(E_T)e^{-E_T/k_BT}\,dE_T \tag{4}$$

where μ is the reduced mass of the reactants and $g_e = 1/4$ is the electronic statistical factor for the reaction. Other symbols have their usual meanings.

The product branching ratios were estimated using a RRKM (Rice−Ramsperger−Kassel−Marcus) approach. The microcanonical RRKM reaction rate constant of a unimolecular reaction to the product channel, j, is given by[61−63]

$$\kappa_j(E^*) = \frac{\sigma_p N(E^{\neq})}{h\rho(E^*)} \tag{5}$$

Here σ_p is the number of degenerate reaction paths, $N(E^{\neq})$ is the sum of states at the transition state, and $\rho(E^*)$ is the density of states of the CH_3COOH or $CH_2C(OH)_2$ intermediate complex. They were calculated using the Beyer−Swinehart direct count method.[64] Furthermore, the lifetime of intermediate A was estimated by

$$\tau_A(E^*) = \frac{1}{\sum_j \kappa_j(E^*)} \tag{6}$$

where the summation runs over all of the dissociation paths of the intermediate.

All electronic structure calculations on stationary points were carried out using the Gaussian03 program,[65] whereas the energies and forces used in direct dynamics calculations were performed with the MolPro program package.[66]

Results and Discussion

Ab Initio Calculations. For the CH_3 + HOCO reaction, the ab initio calculation results are summarized in Tables 1 and 2. Two minima are labeled as **M₁** for acetic acid (CH_3COOH) and **M₂** for enediol ($CH_2C(OH)_2$). $\mathbf{TS_{H_2O}}$ and $\mathbf{TS_{CH_4}}$ refer to the transition states of CH_3COOH dissociation into the H_2O + CH_2CO and CH_4+ CO_2 products, respectively. The isomerization transition state between the two minima is denoted by $\mathbf{TS_{iso}}$, whereas the dissociation barrier of $CH_2C(OH)_2$ into H_2O + CH_2CO is named $\mathbf{TS_{isw}}$. The structures of these six important stationary points are displayed in Figure 1 and were calculated with the CCSD(T)/aug-cc-pVTZ method. (The Cartesian coordinates of the stationary points are provided in the Supporting Information.[67]) All four transition states involve a hydrogen transfer process. They are tight transition states according to the geometries as well as the high imaginary frequencies.

Table 3 gives a comparison of theoretical relative energetics for the CH_3 + HOCO reaction where the zero-point energy corrections are taken from the CCSD(T)/aug-cc-pVTZ values.

TABLE 2: Vibrational Frequencies (cm^{-1}) and Zero-Point Energies ($kcal \cdot mol^{-1}$) of Stationary Points Involved in the CH_3 + HOCO Reaction Calculated at the CCSD(T)/aug-cc-pVDZ Level of Theory

species	frequencies	zero-point
OH	3684	5.3
H_2O	3905, 3787, 1638	13.3
CO_2	2338, 1315, 659(*e*)	7.1
$^1CH_2$	2961, 2886, 1387	10.3
CH_3	3201(*e*), 3101, 1406(*e*), 499	18.6
CH_4	3144(*t*), 3016, 1535(*e*), 1319(*t*)	27.8
HOCO	3782, 1849, 1252, 1037, 596, 524	12.9
CH_2CO	3303, 3188, 2152, 1400, 1134, 983, 581, 488, 431	19.5
CH_3CO	3131, 3125, 3021, 1858, 1440, 1437, 1333, 1036, 941, 859, 460, 109	26.8
CH_2COOH	3753, 3290, 3172, 1685, 1465, 1355, 1192, 992, 910, 785, 647, 580, 548, 425, 314	30.2
HC(O)OH	3726, 3095, 1776, 1390, 1302, 1111, 1035, 659, 616	21.0
$CH_3C(O)OH$ (**M_1**)	3740, 3169, 3125, 3047, 1793, 1460, 1454, 1400, 1332, 1209, 1052, 991, 857, 650, 574, 542, 413, 75	38.4
$CH_2C(OH)_2$ (**M_2**)	3815, 3799, 3287, 3179, 1751, 1433, 1401, 1245, 1193, 962, 907, 716, 676, 625, 519, 440, 346, 142	37.8
TS_{H_2O}	3763, 3198, 3097, 2033, 1830, 1431, 1340, 1075, 1016, 827, 747, 677, 578, 496, 457, 365, 205, 1917*i*	33.1
TS_{CH_4}	3191, 3118, 2957, 2016, 1781, 1420, 1405, 1271, 1189, 1121, 769, 706, 613, 591, 483, 331, 221, 2061*i*	33.1
TS_{iso}	3733, 3204, 3107, 1946, 1578, 1489, 1396, 1219, 1127, 1049, 973, 785, 719, 614, 547, 485, 412, 2180*i*	34.9
TS_{isw}	3732, 3300, 3187, 2101, 1787, 1425, 1347, 1155, 1015, 982, 755, 694, 619, 603, 562, 427, 385, 1717*i*	34.4

It is clearly shown that the MP2 method gives reasonable results, although there are apparent errors for some species. The CCSD(T) energies also demonstrate that the aug-cc-pVDZ basis set is not large enough to obtain accurate relative energies chemically. However, compared with the aug-cc-pVQZ results, the CCSD(T)/aug-cc-pVTZ results are well converged with a mean error of 0.62 $kcal \cdot mol^{-1}$. The accuracy of the CCSD(T)/aug-cc-pVQZ calculations is supported by comparing them with the available experimental values (0 K), as shown in Table 4. The experimental heats[41−43] of formation in $kcal \cdot mol^{-1}$ are 9.2 ± 0.3 for OH, −57.10 ± 0.01 for H_2O, −93.97 ± 0.01 for CO_2, 93.6 ± 0.6 for $^1CH_2$, 35.8 ± 0.2 for CH_3, −16.0 ± 0.1 for CH_4, −10.8 ± 0.1 for CH_2CO, −0.86 ± 0.4 for CH_3CO, −43.9 ± 0.5 for HOCO, −88.7 ± 0.1 for HC(O)OH, and −99.9 ± 0.4 for $CH_3C(O)OH$.

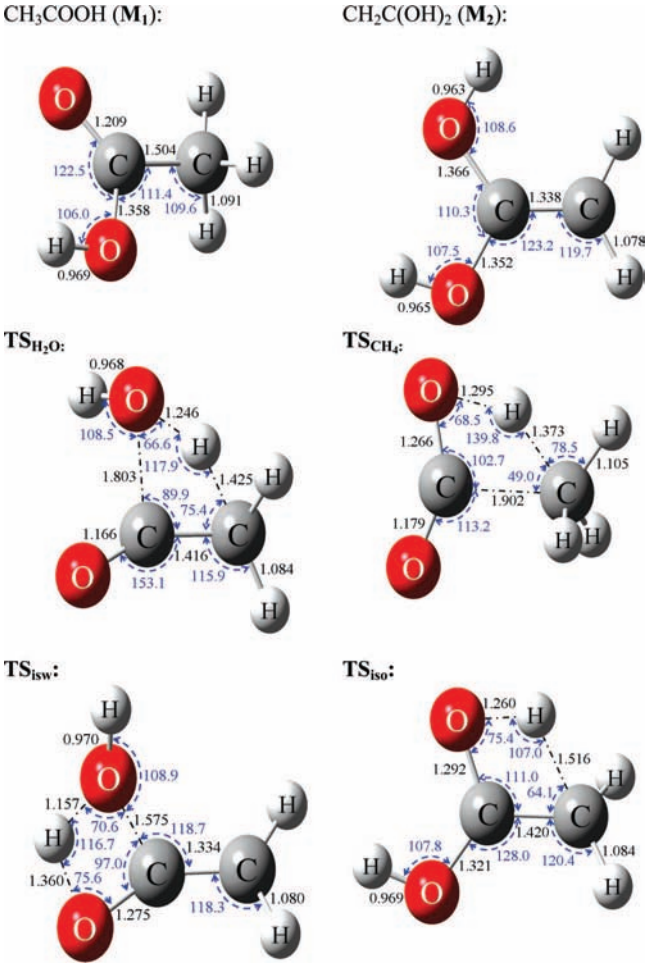

Figure 1. Intermediates and transition states involved in the CH_3 + HOCO reaction. The CCSD(T)/aug-cc-pVTZ structures are labeled in angstroms for bond lengths and degrees for angles.

The reaction pathways are displayed in Figure 2. The CH_3 + HOCO reaction prefers an addition mechanism in which a C−C chemical bond is first formed between two reactants. This results in the production of a stable intermediate, CH_3COOH. Its potential well depth is as large as 98.6 $kcal \cdot mol^{-1}$ at the CCSD(T)/aug-cc-pVQZ level of theory. This complex may break either the C−O bond to produce OH + CH_3CO or the C−C bond to yield $^1CH_2$ + HCOOH via an isomerization reaction. However, both product channels are less likely in energy because of the high barriers. The overall CH_3 + HOCO → OH + CH_3CO (or $^1CH_2$ + HCOOH) reaction is endothermic with a large energy difference of 14.7 $kcal \cdot mol^{-1}$ (or 20.9 kcal). In addition, the CH_3 + HOCO → $^3CH_2$ + HCOOH reaction could occur on the lowest triplet surface. However, it was found that the reaction barrier is high, for example, a value of 16.8 $kcal \cdot mol^{-1}$ estimated with B3LYP/6-31G(d) method. The H + CH_2COOH product channel also lies above the reactants with a relative energy of 9.40 $kcal \cdot mol^{-1}$ at the CCSD(T)/aug-cc-pVQZ method. Therefore, these reactions can be neglected at low temperatures below 1000 K.

On the other hand, the CH_3COOH intermediate can overcome either the **TS_{H_2O}** barrier to dissociate into the H_2O + CH_2CO products or the **TS_{CH_4}** transition state to lead to CH_4 + CO_2, where a hydrogen transfer is involved. (See Figure 1.) Although the barriers are very high, both still lie below the reactant asymptote. Compared with the CH_3+ HOCO → H_2O + CH_2CO reaction, the CH_3+ HOCO → CH_4 + CO_2 reaction will release much more energy. In addition, the barrier height of **TS_{CH_4}** is smaller by 4.1 $kcal \cdot mol^{-1}$ than that of **TS_{H_2O}**. This fact might suggest that the CH_4 + CO_2 products would dominate. Interestingly, it was found that the H_2O + CH_2CO products may be produced through another lower energy pathway. This pathway happens via an isomerization of CH_3COOH to become a less stable $CH_2C(OH)_2$ isomer. In particular, the barrier heights for both the isomerization transition state (**TS_{iso}**) and the dissociation state (**TS_{isw}**) of $CH_2C(OH)_2$ are slightly lower than that of **TS_{CH_4}**. These results really show that the H_2O + CH_2CO products could compete with CH_4 + CO_2 for the CH_3 + HOCO reaction. For

TABLE 3: Relative Energies (Including the Zero-Point Energy Corrections) in kcal·mol^{-1} for the CH_3 + HOCO Reaction

	MP2	CCSD(T)		
species	aug-cc-pVDZ	aug-cc-pVDZ	aug-cc-pVTZ	aug-cc-pVQZ
CH_3 + HOCO	0.0	0.0	0.0	0.0
H_2O + CH_2CO	−61.40	−52.35	−58.84	−59.61
CH_4 + CO_2	−104.45	−98.01	−100.70	−101.48
OH + CH_3CO	16.57	12.40	14.49	15.26
$^1CH_2$ + HCOOH	24.59	20.15	20.62	20.75
H + CH_2COOH	11.48	7.78	9.03	9.40
$CH_3C(O)OH$	−92.98	−88.64	−90.98	−91.71
$CH_2C(OH)_2$	−64.67	−61.10	−64.28	−65.36
$\mathbf{TS_{H_2O}}$	−24.10	−15.07	−16.35	−16.67
$\mathbf{TS_{CH_4}}$	−24.82	−17.27	−20.35	−20.83
$\mathbf{TS_{iso}}$	−22.14	−16.50	−19.59	−20.28
$\mathbf{TS_{isw}}$	−23.01	−17.49	−20.73	−21.22

TABLE 4: Comparison of Theoretical Relative Energies (Including Zero-Point Energy Corrections) in kcal·mol^{-1} with Experimental Results for the CH_3 + HOCO Reaction

	CH_3 + HOCO →				$CH_3C(O)OH$ →				$CH_2C(OH)_2$ →
level of theory	CH_2CO + H_2O	CH_4 + CO_2	HC(O)OH + $^1CH_2$	$CH_3C(O)OH$	$\mathbf{TS_{H_2O}}$	$\mathbf{TS_{CH_4}}$	$\mathbf{TS_{iso}}$	CH_3CO + OH	$\mathbf{TS_{isw}}$
MP2/aug-cc-pVDZ	−61.4	−104.5	24.6	−93.0	68.9	68.2	70.8	109.6	41.7
CCSD(T)/aug-cc-pVDZ	−52.4	−98.0	20.2	−88.7	73.6	71.4	72.1	101.0	43.6
CCSD(T)/aug-cc-pVTZ	−58.9	−100.7	20.6	−91.0	74.6	70.6	71.4	105.5	43.5
CCSD(T)/aug-cc-pVQZ	−59.6	−101.5	20.8	−91.7	75.0	70.9	71.4	107.0	44.1
exptl	−59.8	−101.9		−91.8				108.3	

TABLE 5: Reaction Probabilities (P_r), Cross Sections (σ_r), Product Branching Ratio of H_2O to CH_4 (R_{H_2O/CH_4}), and Lifetimes (τ_A) of the Intermediates CH_3COOH (M_1) and $CH_2C(OH)_2$ (M_2) for the CH_3 + HOCO Reaction

E_T/kcal·mol^{-1}	b_{max}/a_0	N	N_r	P_r	$\sigma_r(\pm\Delta\sigma_r)/a_0^2$	R_{H_2O/CH_4}	τ_{M1}/ns	τ_{M2}/ns
0.5	9.5	956	444	0.4644	131.68(±2.13)	1.54	4.85	0.48
1.0	9.0	604	244	0.4040	102.80(±2.05)	1.56	4.30	0.44
2.5	8.5	900	272	0.3022	68.60(±1.05)	1.64	3.02	0.34
5.0	8.0	584	152	0.2603	52.33(±0.95)	1.77	1.74	0.23
8.0	7.5	660	164	0.2485	43.91(±0.74)	1.91	0.95	0.15
12.0	7.0	772	192	0.2487	38.29(±0.60)	2.10	0.46	0.09

the CH_4 + CO_2 products, another possible reaction pathway is through a direct hydrogen abstraction of CH_3 from HOCO. But our MP2/aug-cc-pVDZ calculations indicate that the classical barrier height is as large as 44.6 kcal·mol^{-1}, which is much larger than the common barrier height of about 18.0 kcal·mol^{-1} for the type of CH_3 + HX (X = H, O, F, Cl, Br, etc.) reactions. Therefore, this pathway is unlikely to be followed.

Dynamics and Kinetics Results. Because the high-level ab initio methods used above are intractable in molecular dynamics studies, we have employed the CAS(4,6)/6-31G(d) method instead. This method was selected as a result of comparing the CAS(4,6) energies of the minimum energy path in the entrance channel for the CH_3 + HOCO reaction with the CCSD(T)/aug-cc-pVTZ and MRCI+Q/cc-pVTZ results. For the capture reaction probability calculations, only the potential energy surface in the entrance channel is important. As shown in Figure 3, the agreement between the two methods is good, which justifies the use of the CAS(4,6)/6-31G(d) in this study. Furthermore, one can notice a very shallow VdW minimum with a binding energy of about 3.9 kcal·mol^{-1} at R_{CC}=7.8a_0. There

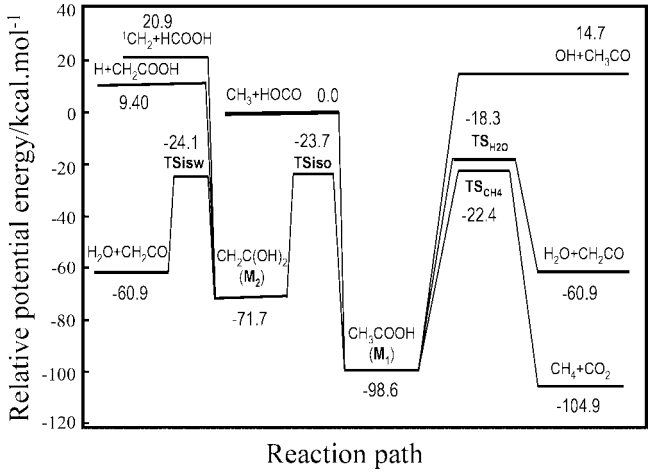

Figure 2. CCSD(T)/aug-cc-pVQZ energy diagram for the reaction pathway of the CH_3 + HOCO reaction.

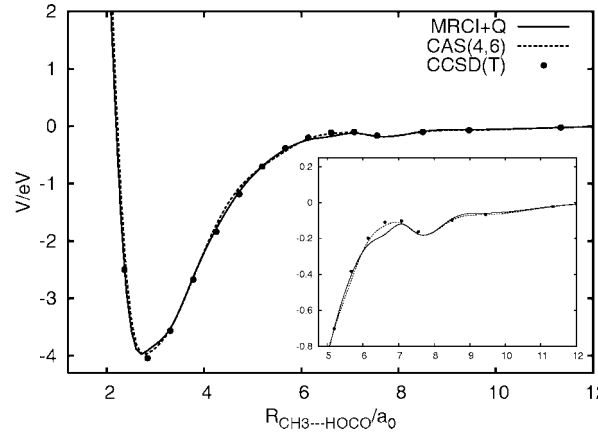

Figure 3. Potential energy curves calculated using CAS(4,6)/6-31G(d), CCSD(T)/aug-cc-pVTZ, and MRCI+Q//CAS(4,6)/cc-pVTZ methods along the CAS(4,6)/6-31G(d) minimum energy path, where the inset is the enlarged part at long ranges.

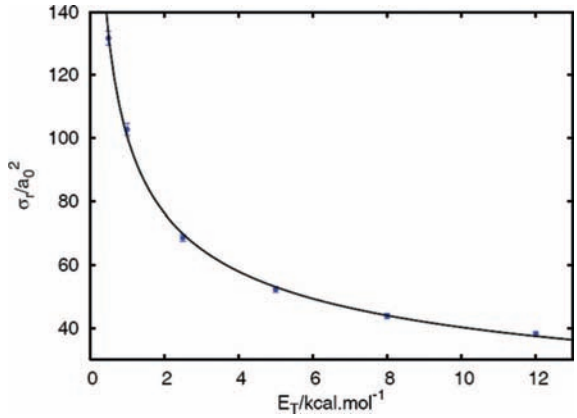

Figure 4. Reaction cross sections as a function of collision energy for the CH_3 + HOCO reaction.

is a loose transition state located at about $R_{CC} = 7.08a_0$ with an energy of about 2.5 kcal·mol^{-1} below the CH_3 + HOCO reactant asymptote. It is well known that such a VdW minimum could substantially enhance the reaction.[68−75]

A total of 4476 trajectories were run at six collision energies in the range between 0.5 and 12.0 kcal·mol^{-1}. The dynamics results are summarized in Table 5. Both the maximum impact parameter and the reaction cross sections decrease as the collision energy increases. This arises from the attractive interaction in the entrance channel for the CH_3 + HOCO reaction so that the long-range interactions play an important role in the dynamical processes. The reaction cross sections are plotted in Figure 4, together with the error bars. The calculated errors are within 2%.

The cross sections sharply increase as the collision energy approaches zero. These results are well fitted by the functional form $\sigma_r(E_T) = \sigma_1/E_T^{\alpha}$, with $\sigma_1 = 100.62 \pm 0.75$ and $\alpha = 0.3976 \pm 0.0076$ in the units of a_0 and kcal·mol^{-1}. The fitted curve is also displayed in the Figure. The agreement is very good. Using this function, we can compute the thermal rate coefficients analytically by[76]

$$k(T) = g_e\left(\frac{8k_BT}{\pi\mu}\right)^{1/2}\left\{\frac{\sigma_1\Gamma(2-\alpha)}{(k_BT)^{\alpha}}\right\} \quad (7)$$

where $\Gamma(x)$ is the Gamma function. The explicit form is $k(T/\mathrm{K}) = 3.24 \times 10^{-11}T^{0.1024}$ in cm^3·molec^{-1}·s^{-1} at temperatures below 1000 K. The thermal rate coefficient is predicted to be 5.80×10^{-11} cm^3·molec^{-1}·s^{-1} with a tiny positive activation energy, $E_a = 0.06$ kcal·mol^{-1}, at room temperature.

Because the OH and CH_2 product channels are inaccessible in energy at the collision energies of interest, there are only two possible product channels: $CH_4 + CO_2$ and OH + CH_3CO. Their product branching ratio at the low pressure limit can be calculated using the following reaction network

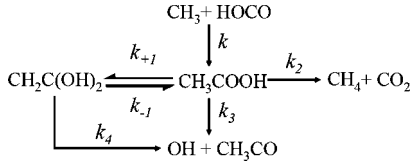

(8)

where we have used the fact that the $CH_3COOH \rightarrow CH_3$ + HOCO backward reaction is negligible because its dissociation barrier height is significantly higher than others in eq 8. By applying the steady state approximation to the metastable $CH_2C(OH)_2$ isomer, the product branching ratio of H_2O to CH_4 is obtained as

$$R_{H_2O/CH_4} = \frac{k_{+1}k_4 + k_3(k_{-1} + k_4)}{k_2(k_{-1} + k_4)} \quad (9)$$

where k_i are the unimolecular reaction rate constants at a given total energy. They are calculated using the RRKM theory described above. The results obtained are listed in Table 5.

The results show that both CH_3COOH and $CH_2C(OH)_2$ are long-lived intermediates with a lifetime on the order of nanoseconds. This may imply that the RRKM approach is a good approximation for determining the product branching ratio. Indeed, the long-lived intermediates are consistent with the feature of deep wells on the potential energy surface of the system. In particular, the $CH_2C(OH)_2$ lifetime is about one order shorter than that of CH_3COOH so that the steady state approximation will work well.

The product branching ratios weakly depend on the collision energy, E_T. They can be represented by a linear function, $R_{H_2O/CH_4} = 1.52 + 0.049E_T$, where the energy is in the kilocalories per mole. The corresponding temperature-dependent ratios are obtained as $R_{H_2O/CH_4}(T/\mathrm{K}) = 1.52 + (1.95 \times 10^{-4})T$. At room temperature, the ratio of H_2O to CH_4 is 1.58, or a fraction of 0.61 for $H_2O + CH_2CO$ and of 0.39 for $CH_4 + CO_2$. In other words, the CH_3 + HOCO reaction produces more $H_2O + CH_2CO$ products rather than the most exothermic products $CH_4 + CO_2$. Actually, it is not surprising according to the competitive reaction pathways mentioned in Ab Initio Calculations section.

Summary

The CH_3 + HOCO reaction has been explored using the CCSD(T) theory with large basis sets. The ab initio calculations show that the reaction occurs via an addition reaction mechanism through long-lived complexes. At low collision energies of < 15.0 kcal·mol^{-1}, there are only two possible product channels: $CH_4 + CO_2$ and $H_2O + CH_2CO$. The reaction rate coefficients were computed using a direct ab initio molecular dynamics approach. The results predict a fast radical−radical reaction. At room temperature, the thermal rate coefficient obtained is 5.80×10^{-11} cm^3·molec^{-1}·s^{-1} with an activation energy (E_a) of 0.06 kcal·mol^{-1}. In addition, the RRKM theory has been employed in determining the product branching ratios. Although the CH_3 + HOCO → $CH_4 + CO_2$ reaction is more thermodynamically favorable, the CH_3 + HOCO → $H_2O + CH_2CO$ reaction is more kinetically favorable.

Acknowledgment. This work was performed at Brookhaven National Laboratory under contract no. DE-AC02-98CH10886 with the U.S. Department of Energy and supported by its Division of Chemical Sciences, Office of Basic Energy Sciences. Some calculations were carried out at the National Energy Research Scientific Computing Center (NERSC) at Lawrence Berkeley National Laboratory.

Supporting Information Available: Cartesian coordinates in angstroms of stationary points involved in the CH_3 + HOCO reaction, optimized at the CCSD(T)/aug-cc-PVDZ level of theory. This material is available free of charge via the Internet at http://pubs.acs.org.

References and Notes

(1) Pilling, M. J. *Annu. Rev. Phys. Chem.* **1996**, *47*, 81.
(2) Wang, B. S.; Hou, H.; Yoder, L. M.; Muckerman, J. T.; Fockenberg, C. *J. Phys. Chem. A* **2003**, *107*, 11414.

(3) Fernandes, R. X.; Luther, K.; Troe, J. *J. Phys. Chem. A* **2006**, *110*, 4442.
(4) Pacey, P. D. *J. Phys. Chem. A* **1998**, *102*, 8541.
(5) Jasper, A. W.; Klippenstein, S. J.; Harding, L. B.; Ruscic, B. *J. Phys. Chem. A* **2007**, *111*, 3932.
(6) Klippenstein, S. J.; Harding, L. B. *J. Phys. Chem. A* **1999**, *103*, 9388.
(7) Tonokura, K.; Ogura, T.; Koshi, M. *J. Phys. Chem. A* **2004**, *108*, 7801.
(8) Goos, E.; Hippler, H.; Kachiani, C.; Svedung, H. *Phys. Chem. Chem. Phys.* **2002**, *4*, 4372.
(9) Knyazev, V. D.; Slagle, I. R. *J. Phys. Chem. A* **2001**, *105*, 6490.
(10) Scire, J. J.; Yetter, R. A.; Dryer, F. L. *Int. J. Chem. Kinet.* **2001**, *33*, 75.
(11) Thorn, R. P., Jr.; Payne, W. A., Jr.; Chillier, X. D. F.; Stief, L. J.; Nesbitt, F. L.; Tardy, D. C. *Int. J. Chem. Kinet.* **2000**, *32*, 304.
(12) Fahr, A.; Laufer, A. H.; Tardy, D. C. *J. Phys. Chem. A* **1999**, *103*, 8433.
(13) Hwang, S. M.; Ryu, S.-O.; De Witt, K. J.; Rabinowitz, M. J. *J. Phys. Chem. A* **1999**, *103*, 5949.
(14) Naroznik, M. *J. Chem. Soc., Faraday Trans.* **1998**, *94*, 2531.
(15) Baeck, H. J.; Shin, K. S.; Yang, H.; Qin, Z.; Lissianski, V.; Gardiner, W. C., Jr. *J. Phys. Chem.* **1995**, *99*, 15925.
(16) Diau, E. W.; Lin, M. C. *Int. J. Chem. Kinet.* **1995**, *27*, 855.
(17) Kaiser, E. W. *J. Phys. Chem.* **1993**, *97*, 11681.
(18) Fagerström, K.; Lund, A.; Mahmoud, G.; Jodkowski, J. T.; Ratajczak, E. *Chem. Phys. Lett.* **1993**, *204*, 226.
(19) Oser, H.; Stothard, N. D.; Humpfer, R.; Grotheer, H. H. *J. Phys. Chem.* **1992**, *96*, 5359.
(20) Anastasi, C.; Beveron, S.; Ellermann, T.; Pagsberg, P. *J.Chem. Soc., Faraday Trans.* **1991**, *87*, 2325.
(21) Smith, I. W. M. *Chem. Phys. Lett.* **1977**, *49*, 112.
(22) Frost, M. J.; Sharkey, P.; Smith, I. W. M. *J. Phys. Chem.* **1993**, *97*, 12254.
(23) Petty, J. T.; Harrison, J. A.; Moore, C. B. *J. Phys. Chem.* **1993**, *97*, 11194.
(24) Schatz, G. C.; Dyck, J. *Chem. Phys. Lett.* **1992**, *188*, 11.
(25) Kudla, K.; Schatz, G. C. *J. Phys. Chem.* **1991**, *95*, 8267.
(26) Medvedev, D. M.; Gray, S. K.; Goldfield, E. M.; Lakin, M. J.; Troya, D.; Schatz, G. C. *J. Chem. Phys.* **2004**, *120*, 1231.
(27) Lakin, M. J.; Troya, D.; Schatz, G. C.; Harding, L. B. *J. Chem. Phys.* **2003**, *119*, 5848.
(28) Troya, D.; Lakin, M. J.; Schatz, G. C.; Harding, L. B.; González, M. *J. Phys. Chem. B* **2002**, *106*, 8148.
(29) Lester, M. I.; Pond, B. V.; Marshall, M. D.; Anderson, D. T.; Harding, L. B.; Wagner, A. F. *Faraday Discuss.* **2001**, *118*, 373.
(30) Pond, B. V.; Lester, M. I. *J. Chem. Phys.* **2003**, *118*, 2223.
(31) Marshall, M. D.; Pond, B. V.; Lester, M. I. *J. Chem. Phys.* **2003**, *118*, 1196.
(32) Dixon, D. A.; Feller, D.; Francisco, J. S. *J. Phys. Chem. A* **2003**, *107*, 186.
(33) Clements, T. G.; Continetti, R. E.; Francisco, J. S. *J. Chem. Phys.* **2002**, *117*, 6478.
(34) Sun, H. Y.; Law, C. K. *J. Mol. Struct.: THEOCHEM.* **2008**, *862*, 138.
(35) Chen, W. C.; Marcus, R. A. *J. Chem. Phys.* **2006**, *124*, 024306.
(36) Yu, H.-G.; Muckerman, J. T.; Sears, T. J. *Chem. Phys. Lett.* **2001**, *349*, 547.
(37) Feilberg, K. L.; Sellevåg, S. R.; Nielsen, C. J.; Griffith, D. W. T.; Johnson, M. S. *Phys. Chem. Chem. Phys.* **2002**, *4*, 4687.
(38) Senosiain, J. P.; Klippenstein, S. J.; Miller, J. A. *Proc. Combust. Inst.* **2005**, *30*, 945.
(39) Larson, C. W.; Stewart, P. H.; Golden, D. M. *Int. J. Chem. Kinet.* **1988**, *20*, 27.
(40) Garcia, E.; Saracibar, A.; Zuazo, L.; Laganà, A. *Chem. Phys.* **2007**, *332*, 162.
(41) Rusic, B.; Boggs, J. E.; Burat, A. *J. Phys. Chem. Ref. Data* **2005**, *34*, 573.
(42) Chao, J.; Zwolinski, B. J. *J. Phys. Chem. Ref. Data* **1978**, *7*, 363.
(43) Hunnicutt, S. S.; Waits, C. D.; Guest, J. A. *J. Phys. Chem.* **1989**, *93*, 5188.
(44) Li, Q.; Osborne, M. C.; Smith, I. W. M. *Int. J. Chem. Kin.* **2000**, *32*, 85.
(45) Yu, H.-G.; Francisco, J. S.; Muckerman, J. T. *J. Chem. Phys.* **2008**, *129*, 064301.
(46) Yu, H.-G.; Francisco, J. S. *J. Chem. Phys.* **2008**, *128*, 244315.
(47) Yu, H.-G.; Muckerman, J. T.; Francisco, J. S. *J. Chem. Phys.* **2007**, *127*, 094302.
(48) Moller, C.; Plessef, M. S. *Phys. Rev.* **1934**, *46*, 618.
(49) Pople, J. A.; Binkley, J. S.; Seeger, R. *Int. J. Quantum Chem., Symp.* **1976**, *10*, 110.
(50) Dunning, T. H., Jr. *J. Chem. Phys.* **1989**, *93*, 1007.
(51) Kendell, R. A.; Dunning, T. H., Jr.; Harrison, R. J. *J. Chem. Phys.* **1992**, *96*, 6796.
(52) Woon, D. E., Jr. *J. Chem. Phys.* **1993**, *98*, 1358.
(53) Schlegel, H. B. *J. Comput. Chem.* **1982**, *3*, 214.
(54) Watts, J. D.; Gauss, J.; Bartlett, R. J. *J. Chem. Phys.* **1993**, *98*, 8718.
(55) Scuseria, G. E.; Lee, T. J. *J. Chem. Phys.* **1990**, *93*, 5851.
(56) Yu, H.-G.; Muckerman, J. T. *J. Phys. Chem. A* **2004**, *108*, 8615.
(57) Yu, H.-G.; Muckerman, J. T. *J. Phys. Chem. A* **2005**, *109*, 1890.
(58) Yu, H.-G. *J. Chem. Phys.* **2008**, *128*, 194106.
(59) Werner, H.-J.; Knowles, P. J. *J. Chem. Phys.* **1985**, *82*, 5053.
(60) Hase, W. L. In *Encyclopedia of Computational Chemistry*; Schleyer, P. v. R., Ed.; John Wiley: New York, 1998.
(61) Hase, W. L. *Acc. Chem. Res.* **1983**, *16*, 258.
(62) Bare, T.; Hase, W. L. *Unimolecular Reaction Dynamics: Theory and Experiments*; Oxford University Press: New York, 1996.
(63) Fernandez-Ramos, A.; Miller, J. A.; Klippenstein, S. T.; Truhlar, D. G. *Chem. Rev.* **2006**, *106*, 4518.
(64) Bryer, T.; Swinehart, D. R. *Commun. ACM* **1973**, *16*, 379.
(65) Frisch, M. J.; Trucks, G. W.; Schlegel, H. B.; Scuseria, G. E.; Robb, M. A.; Cheeseman, J. R.; Montgomery, J. A., Jr.; Vreven, T.; Kudin, K. N.; Burant, J. C.; Millam, J. M.; Iyengar, S. S.; Tomasi, J.; Barone, V.; Mennucci, B.; Cossi, M.; Scalmani, G.; Rega, N.; Petersson, G. A.; Nakatsuji, H.; Hada, M.; Ehara, M.; Toyota, K.; Fukuda, R.; Hasegawa, J.; Ishida, M.; Nakajima, T.; Honda, Y.; Kitao, O.; Nakai, H.; Klene, M.; Li, X.; Knox, J. E.; Hratchian, H. P.; Cross, J. B.; Bakken, V.; Adamo, C.; Jaramillo, J.; Gomperts, R.; Stratmann, R. E.; Yazyev, O.; Austin, A. J.; Cammi, R.; Pomelli, C.; Ochterski, J. W.; Ayala, P. Y.; Morokuma, K.; Voth, G. A.; Salvador, P.; Dannenberg, J. J.; Zakrzewski, V. G.; Dapprich, S.; Daniels, A. D.; Strain, M. C.; Farkas, O.; Malick, D. K.; Rabuck, A. D.; Raghavachari, K.; Foresman, J. B.; Ortiz, J. V.; Cui, Q.; Baboul, A. G.; Clifford, S.; Cioslowski, J.; Stefanov, B. B.; Liu, G.; Liashenko, A.; Piskorz, P.; Komaromi, I.; Martin, R. L.; Fox, D. J.; Keith, T.; Al-Laham, M. A.; Peng, C. Y.; Nanayakkara, A.; Challacombe, M.; Gill, P. M. W.; Johnson, B.; Chen, W.; Wong, M. W.; Gonzalez, C.; Pople, J. A. *Gaussian 03*, revision B.04; Gaussian, Inc.: Wallingford, CT, 2004.
(66) MOLPRO is package of ab initio programs for molecular electronic structure calculations, written by H.-J. Wener and P. J. Knowles and containing contributions from a number of other authors.
(67) See the supplementary material for the Cartesian coordinates in angstroms of stationary points involved in the CH_3 + HOCO reaction, optimized at the CCSD(T)/aug-cc-PVDZ level of theory.
(68) Russell, J. J.; Steetula, J. A.; Gutman, D. *J. Am. Chem. Soc.* **1988**, *110*, 3092.
(69) Nicovich, J. M.; van Dijk, C. A.; Kreutter, K. D.; Wine, P. H. *J. Phys. Chem.* **1991**, *95*, 9890.
(70) Seakins, P. W.; Pilling, M. J.; Niiranen, J. T.; Gutman, D.; Krasnoperov, L. N. *J. Phys. Chem.* **1992**, *96*, 9847.
(71) Krasnoperov, L. N.; Mehta, K. *J. Phys. Chem. A* **1999**, *103*, 8008.
(72) Chen, Y.; Rauk, A.; Tschuikow-Roux, E. *J. Phys. Chem.* **1991**, *95*, 9900.
(73) Yu, H.-G.; Nyman, G. J. *Chem. Phys.* **1999**, *111*, 6693.
(74) Yu, H.-G.; Nyman, G. J. *Chem. Phys.* **2000**, *113*, 8936.
(75) Yu, H.-G.; Nyman, G. J. *Phys. Chem. A* **2001**, *105*, 2240.
(76) Silveira, D. M.; Caridade, P. J. S. B.; Varandas, A. J. C. J. *Phys. Chem. A* **2004**, *108*, 8721.

JP809730J